Pergamon

Cement and Concrete Research 30 (2000) 1427–1433

CEMENT AND CONCRETE RESEARCH

Effect of water/cement ratio and silica fume addition on the fracture toughness and morphology of fractured surfaces of gravel concretes

G. Prokopski[a,*], B. Langier[b]

[a]*Rzeszów University of Technology, Powstańców Warszawy 6, 35-959 Rzeszów, Poland*
[b]*Technical University of Częstochowa, Akademicka 3, 42-200 Częstochowa, Poland*

Received 12 November 1999; accepted 5 June 2000

Abstract

The results of the fracture toughness investigations for concretes made from natural gravel aggregate, with diverse water/cement ratio (W/C = 0.33, 0.43, 0.53 and 0.63), without silica fume and with a silica fume addition are discussed. The critical values of the stress intensity factor, K_{Ic}^{S}, as well as, the critical values of crack tip opening displacement, $CTOD_c$ were determined. Also, the examination results for profile roughness parameter, R_L, and fractal dimension, D, of concrete specimen fractures obtained in fracture toughness tests were performed. The largest values of the stress intensity factor, K_{Ic}^{S}, were showed by concretes with the lowest water/cement ratio, W/C=0.33 (both with and without silica fume addition). This was caused by considerably lower porosity of the aggregate–cement paste transition zone as observed in microstructural examinations, which had in this case a compact structure with a small number of structural defects. Cracks, upon reaching the critical force P_Q, ran through the coarse aggregate grains, and the obtained fractures were flat in character. The examined parameters of fracture morphology, i.e., the profile line development degree, R_L, and the fractal dimension, D, reached the smallest values for those fractures. As the water/cement ratio increased, an increase in the structural porosity of the aggregate–cement paste transition zone occurred, which caused a promoted propagation of cracks and resulted in the obtaining of lower values of stress intensity factor, K_{Ic}^{S}. Cracks in this case propagated avoiding coarse gravel grains (an overgrain fracture formed), which resulted in increased fracture surface roughness and in a rise of the values of both examined parameters of fracture surface morphology, R_L and D.

Keywords: Interfacial transition zone; Fracture toughness; Silica fume; Concrete

1. Introduction

Concrete is a multi-phase material, which makes its properties impossible to be determined without an analysis of the effect of its individual components on the service properties and designation for various applications. Being the most common material in building construction, concrete is continuously subject to intensive and comprehensive investigations.

Of the factors that influence the properties of concrete, particular importance is attributed to the aggregate–cement paste transition layer that is regarded as the most sensitive area within the structure of concrete. The structure of the transition zone, and thus its properties, are influenced by several factors, such as the type of components used (coarse aggregate, cement, additions and admixtures) and the water–cement ratio. A particularly significant role is attributed to the latter of the above factors, which has been confirmed by numerous studies in which an increased porosity has been found to occur in the area of the aggregate–cement paste interface caused by the higher water/cement ratio in this region with a simultaneous decrease in water/cement in the bulk of the matrix [1,2].

The examinations of the matrix structure clearly indicate the occurrence of porosity gradient with the maximum at the surface of the aggregate grains [3–5]. The cause of the increased porosity and the related properties of the transition zone are ascribed by many researchers to water/cement ratio.

According to Ref. [6], the structure of porosity of the transition zone, its thickness and properties, are all closely

* Corresponding author. Tel.: +48-17-865-1439; fax: +48-17-854-3365.
E-mail address: grzeprok@ewa.prz.rzeszow.pl (G. Prokopski).

0008-8846/00/$ – see front matter
PII: S0008-8846(00)00332-X

related to water/cement ratio. Ref. [7] reports that the local increase in water/cement in the area of the aggregate–cement paste interface is proportional to the amount of free unbound water, and any action increasing the contents of the solid phase reduces the effect of the transition zone on the strength properties of concrete. According to Ref. [8], water/cement has little effect on the transition zone thickness, while substantially influencing its porosity.

The increase in water/cement at the surface of aggregate grains is most commonly explained by the so-called "wall effect" caused by the difference in the grain size between aggregate and cement.

The evaluation of the effect of the transition zone on the strength properties of concretes has been increasingly performed in recent years. While applying for this purpose, studies utilising the methods of fracture mechanics that relate the obtained strength parameters to the structural defects (primary cracks) which, in the case of concretes, are unavoidable. It results from the microstructural studies (e.g., Ref. [9]) that it is the transition zone, and specifically, the aggregate–cement paste interface, where the greatest number of defects occur, and that the concrete failure process commences at the transition zone.

The morphology of the fracture surface occurring in the fracture process is a function of the material structure and, in the case of concrete, depends on the properties of the particular components and their sieving curves, the spatial configuration and interaction of phases, as well as on many interdependent mechanical and physical conditions of the failure process.

In order to determine the actual relationships between the structure and mechanical properties of concretes, it is necessary to use fractal geometry to describe the surface of fractures. This is caused by the strong irregularities of the fracture surfaces of concretes, which makes traditional Euclidean geometry unsuitable for this purpose.

The use of fractal analysis for describing the fracture surface of concretes is a relatively new research method (as compared to its use for, e.g., metals). This method has proved very effective because of the strong inhomogeneity of concretes [10–15].

The development of fractal geometry was initiated by Mandelbrot [16,17], who worked out the theoretical bases for the description of irregular (self-similar) curves and introduced the concept of "fractal" (Lat. *fractus* — broken, made up of fractions) to many branches of science.

Fractal dimension is defined by the relationship corresponding to the segment of the line from which the fractal line is generated [Eq. (1)] [16]:

$$D = \frac{\ln N}{\ln(1/r)} \text{ or } N = (1/r)^D \quad (1)$$

where N is the number of sub-parts for which the initial segment of unit length is divided at each step, r is the length of each sub-part, $1/r$ is the scaling factor.

Fractal dimension D characterizes the irregularity of fractal objects. A straight line has a fractal dimension $D=1$, a curve has a fractal dimension D contained between the values 1 and 2, depending on the degree of its development, whereas for surfaces fractal dimension lies in the range from 2 to 3. The more irregular object, the greater is its fractal dimension D.

The generation of a fractal line may be repeated indefinitely and the total length of the line is expressed as a function of r and D by the following relationship [Eq. (2)]:

$$L = L_o r^{-(D-1)} \quad (2)$$

where L is actual length of profile line and L_o is the length of the initial straight segment.

The problem of the description of fracture morphology (in studies on steels) was dealt with, among others, Pickens and Gurland [18], who proposed profile roughness parameter, R_L, as another measure of fracture roughness, defined as the relation of the actual fracture line length, L, to the length of its projection onto the reference line, L_o [Eq. (3)]:

$$R_L = L/L_o \quad (3)$$

The characterization of the fracture surface after the analysis of profiles is based on an assumption that having determined the profile roughness parameter, R_L, it is possible to define the fracture roughness parameter [Eq. (4)]:

$$R_S = S/S_o \quad (4)$$

where S is actual fracture area and S_o is the apparent projected area, and projection is on the mean or average topographic plane.

A practical method of performing the examination of fractal fracture surfaces as obtained from fracture toughness tests, using a digitizer and an IBM PC computer is described, e.g., in Ref. [14].

Despite the fact that the problem of the effect of the transition zone on the properties of concretes has been intensively investigated by numerous researchers, no single model has been developed so far, which would explain the cause for the formation of the transition zone; also, it has not been established how great the effect of this zone is on the properties of concretes.

2. Purpose and scope of the examinations

The paper presents the results of studies on the effects of the water/cement ratio and silica fume addition on the fracture toughness of gravel concrete. Fracture toughness tests were performed using Mode I (tension at bending) according to the RILEM Draft Recommendations [19]. The critical values of stress intensity factors, $K_{Ic}{}^{S}$, and critical crack tip opening displacement, $CTOD_c$, were determined.

The concrete mixtures were prepared from Portland cement with "35" grade additions supplied by Rudniki

Table 1
Compositions of the concrete mixtures and their average compressive strengths

Concrete type	GA	GB	GC	GD
W/C	0.43	0.53	0.63	0.33
Mixture composition, [kg]:				
Cement	357	357	357	357
Aggregate	1911	1911	1911	1911
Water	155	191	226	119
Plasticizer	–	–	–	3.3% of cement mass
Compressive strength, $\bar{R}_c$ [MPa]	56.0	47.2	32.4	63.8

Concrete type	GMA	GMB	GMC	GMD
W/C	0.43	0.53	0.63	0.33
Mixture composition, [kg]:				
Cement	357	357	357	357
Aggregate	1876	1876	1876	1876
Water	155	191	226	119
Silica fume	35	35	35	35
Plasticizer	–	–	–	3.3% of cement mass
Compressive strength, $\bar{R}_c$ [MPa]	62.5	51.1	40.2	73.7

Cement Plant at Częstochowa (Poland), 0÷2 mm sand, gravel with a grain size of up to 16 mm, and superplasticizer. Four batches of concrete mixtures were prepared with the following water/cement ratios: series GA — W/C = 0.33; series GB — W/C = 0.43; series GC — W/C = 0.53; series GD — W/C = 0.63. The concrete mixture of the basic series GB (W/C = 0.43) was designed as an experimental method as a plastic mixture.

Also, four series of concrete mixtures were made with an addition of 10% silica fume (series GMA, GMB, GMC, and GMD), with the same water/cement ratios as those in the previous mixtures. The silica fume constituted 10% of the cement mass, and was a replacement for fine aggregate, i.e., it reduced the sand mass by 10%. In those mixtures, the sand point of the aggregate mixture was maintained constant at 30%.

A superplasticizer was added to the GA and GMA series mixture. The compositions of the concrete mixtures and the results of the compressive strength tests are summarised in Table 1.

From each concrete mixture, five 0.15 m sample cubes were prepared for compressive tests, and six 0.7 × 0.15 × 0.08 m beams with a single initial crack for testing according to Mode I of fracture (according to Ref. [19]). The initial cracks were made by the insert-moulding of 3 mm-thick steel blades with an apex angle of approximately 25°. The specimens were unmoulded after 24 (cubes) and 48 h (beams), and then cured in laboratory conditions until reaching the age of 28 days.

3. Fracture toughness tests

Tests according to Mode I of fracture were carried out using test specimen with dimensions as given in the RILEM Draft Recommendations [19]: W=150 mm, b=80 mm, L=700 mm, S=600 mm, a_o=50 mm (Fig. 1).

An MTS 810 hydraulic testing machine was used in the tests. Loading rate was selected so that the maximum load was reached in approximately 5 min. The applied load was reduced at approximately 95% post-peak load. After reducing the load to zero, the test specimen was loaded again. For each test specimen, six to eight loading–unloading cycles were completed, while recording plots of the loading force as a function of crack mouth opening displacement (CMOD). An example plot of CMOD vs. load increment is shown in Fig. 2. Based on the plots obtained for each test specimen, the following quantities were determined: Young's modulus, E; critical effective crack length, a_c; critical stress intensity factor, K_{Ic}^S, and critical $CTOD_c$.

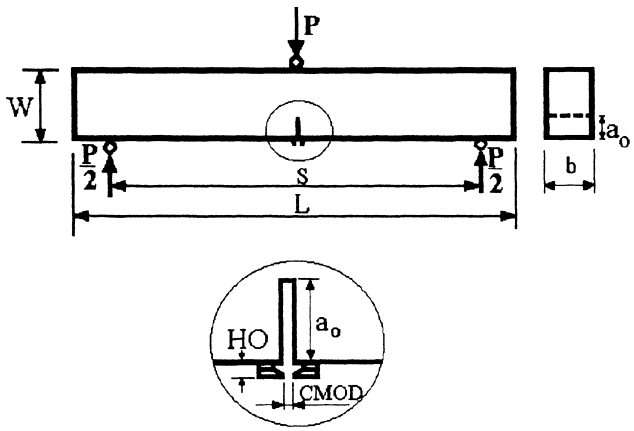

Fig. 1. Schematic drawings of the specimen used in the fracture toughness examination according to Mode I, HO — clamp gauge holder thickness, CMOD — crack mouth opening displacement.

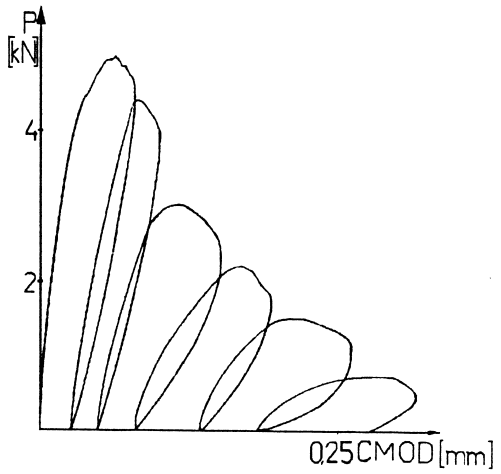

Fig. 2. An example graph of CMOD–load relationship obtained in the tests.

The critical stress intensity factor K_{Ic}^{S} was calculated from the following relationship [Eq. (5)] [19]:

$$K_{Ic}^{S} = 3(P_{max} + 0.5w)\frac{S(\prod a_c)^{1/2}F(\alpha)}{2W^2 b}, \quad (5)$$

in which:

$$F(\alpha) = \frac{1.99 - \alpha(1-\alpha)(2.15 - 3.93\alpha + 2.7\alpha^2)}{\sqrt{\prod^{1/2}(1+2\alpha)(1-\alpha)^{3/2}}},$$

where P_{max}=maximum load, $\alpha = a_c/W$, $w = w_o S/L$, w_o=specimen weight [N], S, a_o, W, b, L — according to Fig. 1.

$CTOD_c$ was determined from the relationship below [Eq. (6)] [19]:

$$CTOD_c = \frac{6P_{max}Sa_cV_1(\alpha)}{EW^2 b} \times [(1-\beta)^2 + (1.081 - 1.149\alpha) \times (\beta - \beta^2)]^{1/2}, \quad (6)$$

where $\beta = a_o/a$ ($a = a_o$ before loading). The results of the tests according to Mode I of fracture are shown in Table 2.

From the obtained test results, relationships of stress intensity factor K_{Ic}^{S} vs. water/cement ratio, W/C, were determined. Figs. 3 and 4 show suitable graphs of regression equations (solid lines), confidence intervals for the regression equations, and confidence intervals for any predictable value of dependent variable as calculated from the regression equations (dotted lines), as well as the average values of the specimen testing results for assumed water/cement ratios.

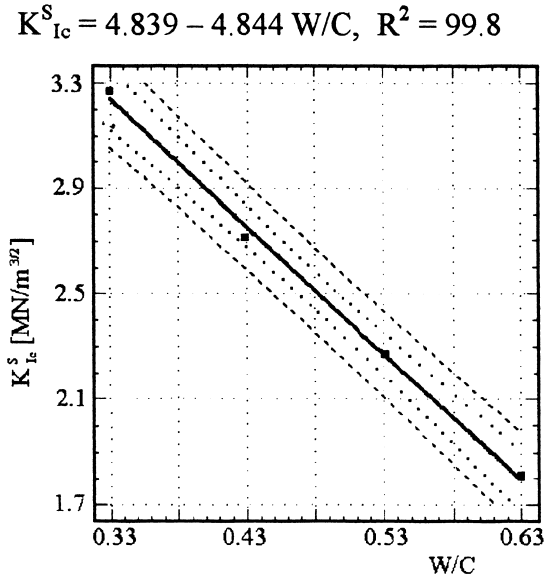

Fig. 3. Relationship of K_{Ic}^{S} vs. W/C (concretes without silica fume).

The performed studies have shown a good sensitivity of stress intensity factor K_{Ic}^{S} to the changes in the aggregate–cement paste transition layer, caused by the change in the water contents of the concrete mixture and addition of silica fume. A clear relationship has been found to exist between water/cement ratio, W/C, and the stress intensity factor K_{Ic}^{S} tested. Increased amount of water in the concrete mixtures caused a significant drop in K_{Ic}^{S}:

- In concretes without silica fume from the value of 3.26 $MNm^{-3/2}$ at W/C=0.33 down to 1.80 $MNm^{-3/2}$ at W/C=0.63 (Fig. 3);
- In concretes with silica fume from the value of 3.57 $MNm^{-3/2}$ at W/C=0.33 down to 2.07 $MNm^{-3/2}$ at W/C=0.63 (Fig. 4).

In Figs. 3 and 4, regression equation graphs (solid lines), regression equation confidence intervals (dotted lines), and

Table 2
Average values of fracture mechanics parameters obtained in the tests

Concrete type	Series GA	Series GB	Series GC	Series GD
K_{Ic}^{S} [$MNm^{-3/2}$] ± s	2.72 ± 0.20	2.28 ± 0.14	1.80 ± 0.09	3.26 ± 0.24
$CTOD_c$ ± s·[10^3 cm]	3.25 ± 0.19	3.71 ± 0.19	2.97 ± 0.22	3.60 ± 0.1
Concrete type	Series GMA	Series GMB	Series GMC	Series GMD
K_{Ic}^{S} [$MNm^{-3/2}$] ± s	2.91 ± 0.25	2.44 ± 0.12	2.07 ± 0.07	3.57 ± 0.16
$CTOD_c$ ± s·[10^3 cm]	3.77 ± 0.43	3.57 ± 0.21	3.41 ± 0.33	3.73 ± 0.19

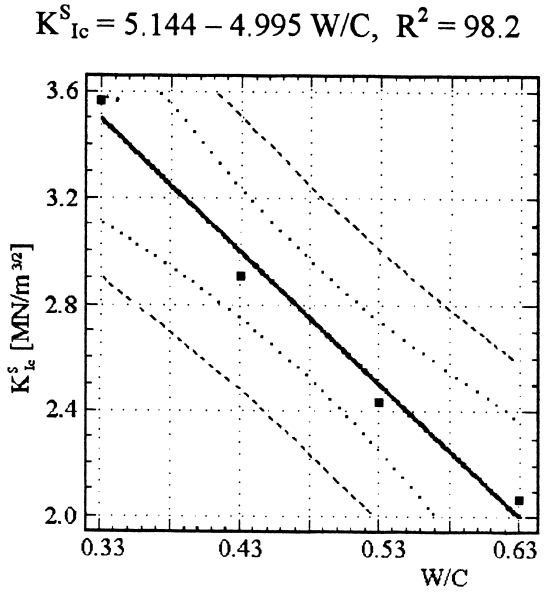

Fig. 4. Relationship of $K_{Ic}{}^S$ vs. W/C (concretes with silica fume).

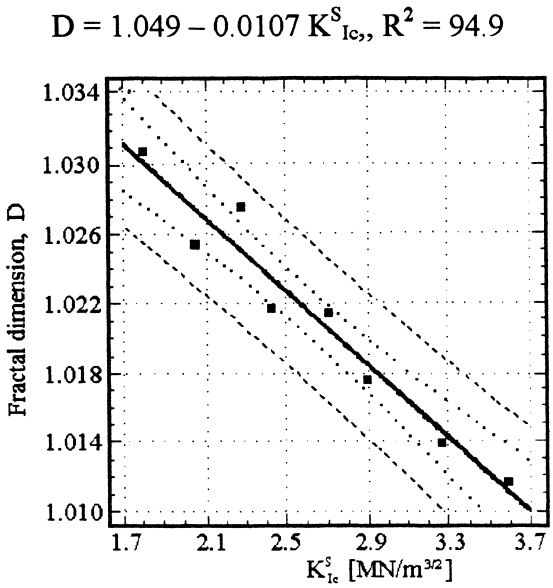

Fig. 5. Dependence of fractal dimension, D, on $K_{Ic}{}^S$.

confidence intervals for an arbitrary expected value of dependent variable as calculated from the regression equations (broken lines) are shown.

The tests for $CTOD_c$ did not reveal a positive relationship between this parameter and the changes in the structure of the aggregate–cement paste transition layer.

4. Fracture morphology examination

The quantitative description of fracture morphology was done based on the analysis of the specimen fracture profile lines obtained in the fracture toughness tests. Subjected to tests were three fractures selected randomly from each series of concretes. White gypsum paste was poured over the obtained fracture surfaces. After the paste had set, a gypsum replica was taken from the concrete fracture, onto which colored gypsum paste was then poured. The replicas were mechanically cut vertically to the mapped fracture surface. The images of replica layers were input to a computer in the form of bitmaps using a scanner. Then, the printout of particular layers was done at a five-time magnification, which enabled the precise mapping of profile lines. Data for the coordinates of profile line generating points were entered to the computer using a digitizer. The digitization process was accomplished using the "operator's point selection" method [20].

Fractal dimension, D, and the actual length of profile lines, R_L, were calculated using the FRACTAL 8 software developed at the Materials Engineering Department of the Technical University of Częstochowa (Poland). The obtained examination results are presented in Table 3. Based on the obtained examination results, the relationships of fractal dimensions, D, and the profile roughness parameter, R_L, have been established as a function of stress intensity factors, $K_{Ic}{}^S$ (Figs. 5 and 6). The dependence of profile

Table 3
Values of profile roughness parameter, R_L, and fractal dimension, D

Concrete type	$K_{Ic}{}^S$ [MNm$^{-3/2}$]	R_L	D
GA	2.72	1.088	1.022
GB	2.28	1.109	1.028
GC	1.80	1.140	1.031
GD	3.26	1.067	1.014
GMA	2.91	1.072	1.018
GMB	2.44	1.093	1.022
GMC	2.07	1.108	1.025
GMD	3.57	1.059	1.012

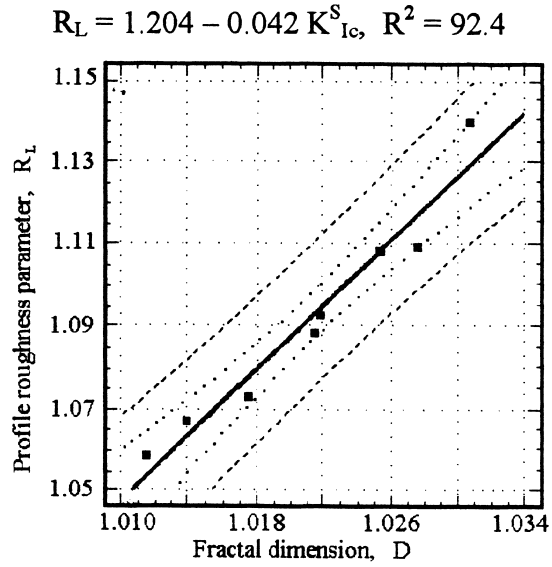

Fig. 6. Dependence of profile roughness parameter, R_L, on $K_{Ic}{}^S$.

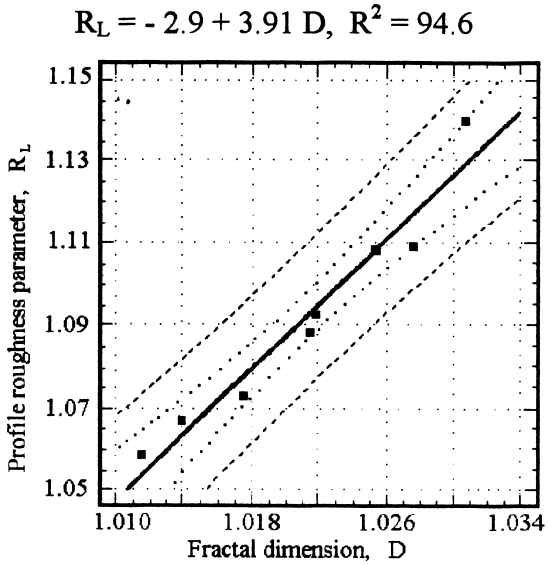

Fig. 7. Dependence of profile roughness parameter, R_L, on fractal dimension D.

roughness parameter, R_L, on fractal dimension, D, has also been determined (Fig. 7).

In Fig. 5, 6 and 7, regression equation graphs (solid lines), regression equation confidence intervals (dotted lines), and confidence intervals for an arbitrary expected value of dependent variable as calculated from the regression equations (broken lines) are shown.

The analysis of fracture surface morphology carried out by utilizing the profile line development degree, R_L, and the fractal dimension, D, has shown a close relationship exists between these parameters and the stress intensity factor, K_{Ic}^S. Larger values of the stress intensity factor, K_{Ic}^S corresponded to lower values of both R_L and D.

In the case of concrete with no silica fume addition, the profile line development degree, R_L, decreased from the value of 1.14 at W/C=0.63 (K_{Ic}^S=1.80 MNm$^{-3/2}$) to the value of 1.067 at W/C=0.33 (K_{Ic}^S=3.26 MNm$^{-3/2}$). The fractal dimension D decreased from the value of 1.031 at W/C = 0.63 to the value 1.014 at W/C=0.33.

For concretes with a silica fume addition, the same trends in the change of both examined parameters were observed. The profile line development degree R_L decreased from the value of 1.093 at W/C=0.63 (K_{Ic}^S=2.07 MNm$^{-3/2}$) to the value of 1.059 at W/C=0.33 (K_{Ic}^S=3.57 MNm$^{-3/2}$). The fractal dimension D decreased from the value 1.025 at W/C=0.63 to the value of 1.012 at W/C=0.33.

5. Conclusions

The studies on the effect of water contents in concrete mixtures and the addition of silica fume using stress intensity factor K_{Ic}^S and morphological examinations are an effective means for the evaluation of the effect of structure changes on the fracture toughness of concretes.

A clear relationship has been found to exist between water/cement ratio (W/C) and the stress intensity factor K_{Ic}^S tested. Increased amount of water in the concrete mixtures caused a significant drop in K_{Ic}^S:

- In concretes without silica fume from the value of 3.26 MNm$^{-3/2}$ at W/C=0.33 down to 1.80 MNm$^{-3/2}$ at W/C=0.63;
- In concretes with silica fume from the value of 3.57 MNm$^{-3/2}$ at W/C=0.33 down to 2.07 MNm$^{-3/2}$ at W/C=0.63.

Addition of silica fume to the concrete mixtures resulted in the enhanced properties of the hardened concrete. Stress intensity factor K_{Ic}^S increased, respectively: for series GMA (W/C=0.33) — by 15%, for series GMB (W/C=0.43) — by 7%, for series GMC (W/C=0.53) — by 9.5%, and for series GMD (W/C=0.63) — by 24%.

The tests for the critical crack tip opening displacement $CTOD_c$ did not reveal a positive relationship between this parameter and the changes in the structure of the aggregate–cement paste transition layer.

Changes in the stress intensity factor K_{Ic}^S are closely related to the changes in the structure of the concretes as observed in the morphological examinations.

Examinations of the fracture surface morphology have shown that the profile roughness parameter, R_L, and fractal dimension, D, of the fracture occurring in the fracture process are closely dependent on the fracture toughness of concrete.

It was found that with increasing stress intensity factor, K_{Ic}^S, profile roughness parameter, R_L, and fractal dimension, D, for both concretes (without and with silica fume) decreased.

The drop in the line development degree R_L and the fractal dimension D with increasing fracture toughness (K_{Ic}^S) of concretes was caused by the increased strength of the aggregate–cement paste transition zone and by larger forces of adhesion of the cement paste to the gravel grains, due to the reduced porosity of this zone (lower both water/cement and the silica fume addition).

In the case of the GA series concrete of (W/C=0.33) and the GMA series concrete (W/C=0.33 with silica fume added), the forces of adhesion of the aggregate to the cement paste were high (higher than the strength of gravel grains), which resulted in the propagation of cracks through the coarse aggregate grains and the formation of flat-surface fractures; the values of R_L and D obtained in the tests were the smallest.

In the case of concretes with a large water/cement ratio (the GD and GMD series), the aggregate–cement paste transition zone was highly porous and weak, which resulted in the development of a crack in this zone; the so-called overgrain fractures, highly irregular and rough, for which

both the profile line development degree R_L and the fractal dimension D had relatively large values.

The obtained relationships of profile roughness parameter, R_L, and fractal dimension D, as a function of stress intensity factor, K_{Ic}^S, as well as the dependence $R_L=f(D)$ show, for a particular concrete, a high level of correlation, which indicates a high susceptibility of the examined fracture morphology parameters, R_L and D, to changes in the structure of concretes and obtained critical values of stress intensity factor, K_{Ic}^S.

The microstructural examinations (see Ref. [21]) showed that the aggregate–cement paste transition zone in concrete from gravel aggregate with a small water/cement ratio (concrete without silica fume addition) and both with a small water/cement ratio and a silica fume addition was uniform and dense, with only a small number of structural discontinuities. A transgranular character of fracture was observed in this case, that its cracks going through the aggregate grains, which caused the formation of a flat fracture surface. The strength of the aggregate–cement paste interface was in this case higher than the strength of gravel grains, which resulted in the critical values of stress intensity factors, K_{Ic}^S, having the greatest values for this series of concrete.

References

[1] E.J. Garboczi, D.P. Bentz, The effect interfacial zone on concrete properties: The dulite limit, in: K.P. Chong, F. Ase (Eds.), Materials for the New Millenium, Fourth Mat. Engin. Conf., Vol. 1, 1996, pp. 1228–1237 Washington.

[2] A.M. Brandt, Cement-based Composites: Materials, Mechanical Properties and Performance, E&FN Spon, London, 1995.

[3] R. Zimbelmann, A contribution to the problem of cement–aggregate bond, Cem Concr Res 15 (1985) 801–808.

[4] A. Bentur, Microstructure, interfacial effects and micromechanics of cementitious composites, Ceram Trans, Vol. 16, The American Ceramic Society, 1991, pp. 523–549.

[5] M.P. Lutz, J.M. Monteiro, Inhomogenous interfacial transition zone model for the bulk modulus of mortar, Cem Concr Res 27 (7) (1997) 1113–1122.

[6] P. Simeonov, S. Ahmad, Effect of transition zone on the elastic behavior of cement-based composites, Cem Concr Res 25 (1) (1995) 165–175.

[7] Ch.Z. Yuan, W.J. Gud, Effect of bond between aggregate and cement paste on the mechanical behaviour of concrete, MRS Symp Proc 114 (1998) 41–47.

[8] D.B. Bentz, E.J. Garboczi, P.E. Stutzman, Computer modelling of the interfacial zone in concrete, Int. RILEM Conf., Toulouse 1992. E&FN Spon, London, 1992, pp. 107–116.

[9] G. Prokopski, Influence of water–cement ratio on micro-cracking of ordinary concrete, J Mater Sci 26 (1991) 6352–6356.

[10] A. Carpinteri, Fractal nature of material microstructure and size effects on apparent mechanical properties, Mech Mater 18 (1994) 89–101.

[11] A.M. Brandt, G. Prokopski, On the fractal dimension of fracture surfaces of concrete elements, J Mater Sci 28 (1993) 4762–4766.

[12] D.N. Winslow, The fractal nature of the surface of cement paste, Cem Concr Res 15 (1985) 817–828.

[13] V.E. Saouma, C.C. Barton, N.A. Gamaleldin, Fractal characterization of concrete crack surfaces, Eng Fract Mech 35 (1) (1990) 47–53.

[14] J.J. Mecholsky, D.E. Passoja, K.S. Feinberg-Ringel, Quantitative analysis of brittle fracture surfaces using fractal geometry, J Am Ceram Soc 72 (1) (1989) 60–65.

[15] B. Chiaia, J.G.M. Mier, A. Vervuurt, Crack growth mechanisms in four different concretes: Microscopic observations and fractal analysis, Cem Concr Res 28 (1) (1998) 103–114.

[16] B.B. Mandelbrot, Les objects fractals, Forme, Hasard et Dimension, Flammarion, Paris, 1975.

[17] B.B. Mandelbrot, The Fractal Geometry of Nature, Freeman, San Francisco, 1982.

[18] J.R. Pickens, J. Gurland, Fourth International Congress of Stereology, Gaithersburg, MD, 1976. (NBS Special Publication).

[19] Determination of fracture parameters (K_{Ic}^S and $CTOD_c$) of plain concrete using three-point bend tests, RILEM Draft Recommendations, TC-89 — FMT Fracture Mechanics of Concrete-Test Methods, Materials and Structures (23) 1990.

[20] L. Wojnar, Quantitative fractography. Basics and computer-aided testing, Scientific Booklets of the Technical University of Cracow, Mechanical Series, Booklet no. 2, Cracow 1990.

[21] G. Prokopski, J. Halbiniak, B. Langier, The examination of the fracture toughness of concretes with diverse structure, J Mater Sci 33 (1997) 1819–1825.